Solar Energy Assessment: From Rooftop Extraction to Identifying Utilizable Areas

Mohammad Aslani[1(✉)] and Stefan Seipel[1,2]

[1] Department of Computer and Geo-spatial Sciences, University of Gävle, Gävle, Sweden
{Mohammad.Aslani,Stefan.Seipel}@hig.se

[2] Division of Visual Information and Interaction, Department of Information Technology, Uppsala University, Uppsala, Sweden

Abstract. Rooftop photovoltaics have been acknowledged as a critical component in cities' efforts to reduce their reliance on fossil fuels and move towards energy sustainability. Identifying rooftop areas suitable for installing rooftop photovoltaics-referred to as utilizable areas-is essential for effective energy planning and developing policies related to renewable energies. Utilizable areas are greatly affected by the size, shape, superstructures of rooftops, and shadow effects. This study estimates utilizable areas and solar energy potential of rooftops by considering the mentioned factors. First, rooftops are extracted from LiDAR data by training PointNet++, a neural network architecture for processing 3D point clouds. The second step involves extracting planar segments of rooftops using a combination of clustering and region growing. Finally, utilizable areas of planar segments are identified by removing areas that do not have a suitable size and do not receive sufficient solar irradiation. Additionally, in this step, areas reserved for accessibility to photovoltaics are removed. According to the experimental results, the methods have a high success rate in rooftop extraction, plane segmentation, and, consequently, estimating utilizable areas for photovoltaics.

Keywords: Rooftop solar energy · Spatial analyses · Plane segmentation · Rooftop extraction · Deep learning

1 Introduction

Rooftop photovoltaics have emerged as a promising solution for satisfying a portion of the energy demand in urban areas owing to their great potential for scalability and lower greenhouse gas emissions. Rooftop photovoltaics allow buildings to become active power producers, reducing their reliance on external energy sources [8]. However, not all rooftop areas are utilizable for photovoltaic deployment. Utilizable rooftop areas are limited by various factors, the most important of which are the shape, orientation, and superstructures of roofs, as well as occlusion [36]. A rooftop with proper orientation and no superstructures or surrounding objects offers high solar energy potential. In contrast, a

C. Grueau et al. (Eds.): GISTAM 2021/2022, CCIS 1908, pp. 102–115, 2023.
https://doi.org/10.1007/978-3-031-44112-7_7

north-facing rooftop with many superstructures surrounded by tall buildings (in the northern hemisphere) may not offer high solar energy potential. Moreover, local climate conditions and geographical location may affect the solar energy potential of rooftops.

Manual identification of utilizable rooftop areas based on the mentioned factors can be time-consuming and even unfeasible, especially for large regions. Hence, more efficient and automated approaches are necessary to expedite the process of identifying utilizable areas. In this context, analyzing LiDAR datasets has been recognized as a potential way to automate this process [15]. LiDAR datasets provide 3D spatial profiles of the area and allow for automatic computation of characteristics of rooftops and their surrounding objects, such as area, height, tilt, and azimuth. The issue of identifying utilizable rooftop areas for photovoltaics installation has been addressed through developing spatially-based methods utilizing geoinformatics. These methods start by outlining the borders of rooftops, modeling their shapes, and identifying areas that are utilizable for rooftop photovoltaics [2,5]. These methods typically take into account the tilt, orientation, and superstructures of rooftops when identifying utilizable areas. In this study, utilizable areas of rooftops are identified using a new spatially-based method.

2 Related Work

2.1 Extraction of Rooftops and Modeling Their Form

Identifying utilizable rooftop areas entails several steps, the first of which is determining the *extent* of rooftops. This step is crucial as it provides information on the overall surface area of rooftops, which can then be used in further analyses to pinpoint utilizable areas. With the fast advancement of remote sensing technologies, point clouds of varying resolutions have become more and more accessible. Consequently, research within the field of automatic building extraction from point clouds has received widespread attention, and many methods have been developed. In these methods, points belonging to rooftops are extracted based on their geometric and morphological features that are different from other objects, such as trees and roads. In this context, a variety of machine-learning approaches have been applied.

In [21], the AdaBoost algorithm was used to classify LiDAR data into four categories: roads, grass, buildings, and trees. Different features, such as height, height variation, and normal vector variation, were used for the classification. Their method was tested on ten regions, and the evaluation results indicated an accuracy of 92%. In [3], support vector machines (SVMs) were employed to identify rooftops. They proposed a new method named data reduction based on locality-sensitive hashing (DRLSH) to automatically select training samples for SVMs. The method was evaluated on a test site in Gothenburg, Sweden, and the results showed its suitable performance. In another study [4], a different instance selection method for SVMs was developed. The method-named border point extraction based on locality-sensitive hashing (BPLSH)- was tested on

several datasets, and the results showed its superiority over other methods. In [33], PointNet++ was used to identify rooftops from LiDAR datasets. It is a deep neural network architecture for 3D point cloud analysis [27]. The authors could accurately identify rooftops in point clouds, showing the potential of this deep learning architecture for 3D data analysis.

Rooftop extraction is required for different spatial applications, but reliable spatial analyses of rooftops require modeling their *shape*. This is particularly important in identifying utilizable areas as the solar suitability of rooftops and the efficiency of photovoltaics rely on rooftops' form. The angle at which a rooftop faces the sun affects the amount of sunlight that photovoltaics receives [40]. Model-driven and data-driven are two commonly used approaches for roof shape modeling.

In the model-driven approach, the rooftop shape is determined based on a predefined library of roof shapes [41]. Indeed, the approach defines a library of roof shapes and chooses a shape that best matches the point cloud or surface model. In [20], this approach was used to model the shape of rooftops in Uppsala. It ensures regularized planar patches and low sensitivity to noise as it incorporates prior knowledge about roof shapes into the modeling process. However, the performance of this approach depends on the defined library's completeness. If the library is not comprehensive enough, it may not accurately represent the rooftop shapes. Moreover, this approach may overlook rooftop superstructures (e.g., chimneys), which play an important role in identifying utilizable areas.

In the data-driven approach, planar segments are derived independently of the overall roof shape [10]. This can be quite beneficial in adhering planar segments to their underlying surface. Furthermore, this approach is not limited to a set of predetermined shapes, and thus it is capable of extracting all planar segments of any arbitrary polyhedral rooftops-including rooftop superstructures [7,16]. Various techniques are commonly utilized in the data-driven approach, such as region growing, random sample consensus (RANSAC), and clustering [38,39].

Region growing is a method to group close pixels with similar characteristics into larger regions or objects. Region growing begins with selecting a number of points (seed points) known to belong to a plane. Then, it iteratively adds neighboring points that meet coplanarity criteria until no more points can be added to the plane. Coplanarity criteria are typically based on measures such as point distance, normal vector difference, and curvature and are used to ensure that the added points are coplanar with the initial seed points. In [18], planar patches of rooftops were segmented using region growing to estimate rooftop solar potential. In [12], a method that replaces points with volumetric elements called voxels was presented to enhance the computational efficiency of region growing. The performance of region growing is greatly affected by how the seeds are arranged and the accuracy of the estimations of surface properties such as normal direction and curvature at various points.

In RANSAC-based methods for plane segmentation, a subset of samples is chosen each time, plane models fit each subset, and the model with the most

inliers is chosen. Inliers are points that lie close to the fitted plane model, while outliers lie far away from the fitted plane model. In [10], RANSAC was used for plane segmentation. Despite the simplicity of classical RANSAC, applying it to plane segmentation in point clouds may result in the detection of spurious planes. Several variations and adaptations of RANSAC have been developed to overcome this issue [38].

Clustering-based methods form planar segments by grouping points with similar features, where the definition of features should enable clear differentiation of planar segments. In a well-defined feature space, points on the same planar segment should be mapped close together. In [31], a clustering-based plane segmentation method based on normal vectors was proposed. The segmentation process uses fuzzy k-means clustering, and a validity index-the degree of compactness and separation of the resulting clusters-is used to obtain the optimal number of clusters. Moreover, a planarity test that distinguishes planar from non-planar points is incorporated to enhance clustering. In [22], density-based spatial clustering of applications with noise (DBSCAN) [13] was used to extract planar segments of rooftops. The feature space for clustering was defined using position, slope, azimuth, and shadow. The choice of clustering algorithm is crucial in this class of methods, and clustering algorithms with high time complexity might be impractical for handling high-resolution point clouds.

2.2 Identification of Rooftop Utilizable Areas

Different factors limit utilizable areas of rooftops for installing photovoltaics [32]. Rooftop superstructures (e.g., chimneys), shadow effects caused by adjacent buildings or trees, and regulations governing the installation of photovoltaics are among the factors that impose limitations [6]. Identifying utilizable areas is critical to avoid overestimating the potential of rooftop solar energy, which could lead to unrealistic expectations and inaccurate planning for integrating solar energy into existing power infrastructures. By considering utilizable areas, developing more informed and realistic strategies for deploying photovoltaics is possible, which can contribute to the transition towards more sustainable energy systems [15,25].

The challenge of identifying utilizable areas has been the subject of numerous studies [9]. A commonly used method for identifying these areas is to use a set of loss coefficients, which indicate the average reduction in available rooftops [29]. These coefficients are determined based on simplified assumptions about rooftops, such as a proportion of rooftops mainly in shadow or used for non-photovoltaic purposes (e.g., air conditioning and accessibility). Although this approach is computationally fast, adapting coefficients to new areas is not trivial, and unsuitable loss coefficients may result in overlooking rooftop variations [35].

To address this issue, a few spatially-based methods have been recently proposed. However, most of the proposed spatially-based methods are limited to manual digitization [11] or simplified roof shape modeling [20], or they may not consider shadow effects [23]. This study identifies utilizable areas with more spatial details by analyzing roof shapes, roof superstructures, and shadow effects. It

aims to automatically (a) extract rooftops using a deep learning-based method, (b) segment planar rooftop patches using a clustering-based method, and (c) identify utilizable areas using morphological operations.

3 Methods

In this section, the procedure for identifying utilizable areas and estimating the solar energy potential of rooftops is detailed. It relies on using LiDAR datasets, which can provide detailed 3D information about an area. It assumes that the LiDAR data has enough density to accurately capture the shape of the rooftops and superstructures that may affect solar energy potential estimates. The major steps of the procedure are explained in the following sections.

3.1 Extraction of Rooftops

The task of rooftop identification falls within the domain of semantic segmentation, in which the objective is to detect points that constitute rooftops. Deep learning methods have made significant progress in recent years and demonstrated impressive results in various semantic segmentation tasks, making them suitable for this purpose. Our study employs PointNet++, a state-of-the-art deep learning architecture designed to handle point cloud data such as LiDAR [27]. PointNet++ is a hierarchical neural network for semantic segmentation of unorganized point data, and it enables multiscale point feature learning. It has the potential to be trained without requiring parameters that are specific to objects in LiDAR. A PointNet++ network consists of sampling, grouping, and mini-PointNet layers. The sampling layer chooses points that form the centroids of local regions. The grouping layer constructs local region sets around the centroids. The mini-PointNet layer abstracts the sets of local features into higher-level representations using a series of convolution, normalization, relu, and max-pooling layers. Please refer to [27] for more details. To effectively train PointNet++ for rooftop extraction, we utilize labeled point cloud datasets encompassing various rooftop features. These labeled datasets provide crucial information on the structure, geometry, and spatial distribution of rooftop points, enabling the network to learn and recognize the distinguishing characteristics of rooftops.

3.2 Rooftop Plane Segmentation

This step involves dividing rooftops into planar or flat regions. It is necessary to identify utilizable areas as planar segments unobstructed by superstructures (e.g., chimneys) provide stable and consistent surfaces for mounting photovoltaics. Plane segmentation is performed on digital surface models (DSMs); thus, the recognized rooftop LiDAR point clouds are converted into DSMs. Planar segments are extracted by clustering, and the feature space for clustering is defined by normal vectors of pixels obtained by fitting a plane to the pixel and its neighbors. Pixels on the same planar segment have similar normal vectors; thus,

planar patches can be identified by grouping them together. Some pixels in each planar segment may, however, have normal vectors that are inconsistent with those of other pixels in the same segment. These pixels are known as non-planar pixels, as they are placed in the vicinity of more than one plane. Including these pixels in clustering may disturb the creation of planar segments since they shatter the boundaries of clusters of normal vectors. As a result, non-planar pixels must be identified and excluded from clustering. Principle component analysis (PCA) is used to evaluate the planarity of each pixel.

To cluster normal vectors, a minimum density divisive clustering (MDDC) algorithm is used [26]. MDDC is a density-based hierarchical clustering algorithm, which assumes continuous regions of low probability density separate clusters. Clusters are formed by hyperplanes that pass through regions with low probability density. The adaptability (i.e., it requires no input parameters) and high computational efficiency of MDDC make it suitable for handling large datasets. Since segmentation using MDDC does not consider the spatial connectivity of pixels, each resulting patch may comprise multiple parallel planar segments that are spatially separated. To split multi-part patches, Euclidean clustering based on pixel coordinates is applied [30]. Finally, the non-planar pixels, initially excluded, are assigned to the best segment using region growing. In this manner, the issue of over-segmentation that could potentially occur during clustering is also addressed.

3.3 Rooftop Utilizable Areas

This stage entails calculating the solar energy potential of rooftops. Since it is not feasible to install photovoltaic panels across the entire rooftop surface, determining the utilizable areas for photovoltaics is crucial to prevent the overestimation of energy generation. Utilizable areas refer to specific rooftop sections where photovoltaic installation is practical. Therefore, every planar segment undergoes a thorough spatial analysis to pinpoint these utilizable areas.

Portions of planar segments need to remain clear of photovoltaics to maintain accessibility, which is an essential requirement for panel installation. Frequently, a gap between the photovoltaic edge and the segment, known as the service area, must be preserved. To exclude these areas, we utilize a morphological erosion operation with a circular structuring element whose radius is equal to the width of the service areas [34]. The erosion operation shrinks the roof face by the width of the service area. In addition to service areas, there might be some areas of planar segments that are too small for a photovoltaic to fit, and these areas should be excluded. To accomplish this, we use morphological opening operations in accordance with Algorithm 1. The inputs to the algorithm include a segment RF_T obtained from the previous step, a structuring element representing a solar panel SP, and a set of angles Δ for rotating the structuring element. The algorithm applies a series of opening operations with varying directions of the structuring element, as solar panels can be installed in different directions in practice. Each iteration identifies regions in the segment that can accommodate

a rotated solar panel through the opening operation. The output RF_{TG} is the merging of all suitable regions obtained over the iterations.

Algorithm 1. Pseudo-code for removing areas that cannot accommodate a solar panel.

Input: A shrunken segment RF_T
A solar panel SP with a size of RPV_{size}
A set of rotation angles $\Delta = \{0°, 10°, 20°, \cdots, 170°\}$
Output: A segment without geometrically unsuitable parts RF_{TG}

$RF_{TG} \leftarrow$ a zero matrix with a size of RF_T
for each $\theta \in \Delta$ **do**
  $SP_\theta \leftarrow$ rotate SP with an angle of θ
  $I_\theta \leftarrow O_{SP_\theta}[RF_T]$ %O_{SP_θ} is an opening operation with structuring element SP_θ
  $RF_{TG} \leftarrow union(RF_{TG}, I_\theta)$
end for
$RF^c_{TG} \leftarrow$ *connected component labeling*(RF_{TG})
for each $RF^r_{TG} \in RF^c_{TG}$ **do**
  if $area(RF^r_{TG}) > area(SP)$ **then**
    Preserve RF^r_{TG}
  end if
end for

Once geometrically incompatible areas have been eliminated; the residual planar segments undergo assessment for solar irradiation. Segments with average solar irradiation falling below a designated threshold SI are excluded, as photovoltaic installations typically avoid rooftop areas with insufficient sunlight. This process helps discard segments predominantly in the shade or those with unfavorable tilts (e.g., excessively steep) or azimuths (e.g., facing north), resulting in the identification of utilizable areas for photovoltaic installation.

By having utilizable areas, the energy potential of rooftops is determined. A rooftop's total solar electricity yield is calculated according to Eq. 1. E is the total solar electricity yield of a rooftop in kWh. S_i and ψ_i are the total solar irradiance (in kWh/m^2) and the tilt angle of the i-th utilizable segment. α and β are the efficiency and performance ratio of the photovoltaics, d is the area of each pixel of the DSM (in m^2), and N is the number of utilizable segments of a rooftop.

$$E = \alpha \cdot \beta \cdot d \cdot \sum_{i=1}^{N} \frac{S_i}{\cos \psi_i} \tag{1}$$

4 Datasets, Results and Discussion

Two datasets are employed in this study to evaluate the performance of the methods. Dayton Annotated LiDAR Earth Scan (DALES) is the first dataset

[37] used to train and evaluate PointNet++ for rooftop extraction. As a publicly accessible resource, DALES offers a comprehensive assortment of LiDAR data from various environments, making it well-suited for deep network training. The dataset encompasses 40 manually labeled scenes. The second dataset encompasses an area within Uppsala city, Sweden, and its LiDAR point cloud was created by the Uppsala municipality. This dataset serves the purpose of plane segmentation and solar energy calculation. To facilitate plane segmentation assessment, we manually identified and labeled planar segments of rooftops and used them as ground truth data. Some scenes from the datasets are shown in Fig. 1.

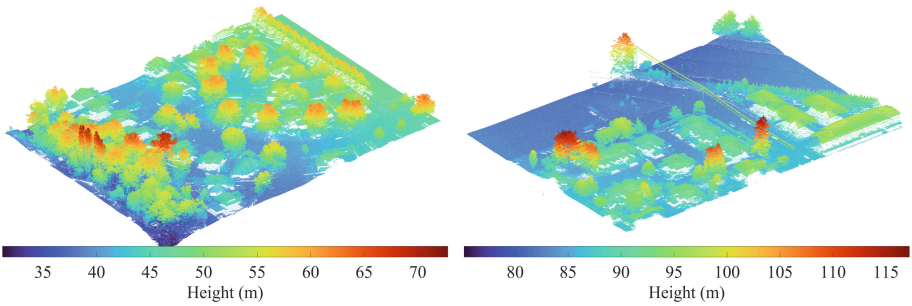

Fig. 1. Some sample scenes from the LiDAR datasets.

The results obtained by applying the procedure to the datasets are presented and discussed. The first step of the procedure is to extract rooftops, which is done by utilizing PointNet++. Of the 40 scenes in the DALES dataset, 29 are designated for training, while the rest serve as test samples. Individual scenes are subdivided into non-overlapping 50-by-50-meter tiles to maximize the dataset's utility. Each tile is then downsampled to contain only 9000 points, speeding up the training process. To train the deep network, the Adam optimizer with a gradient decay rate of 0.9 is used [19]. The maximum number of training epochs is set to 20, with each epoch consisting of 485 iterations. At the beginning of the training, the learning rate is set to 0.0005 and is reduced by a factor of 0.1 in epoch 10. Regularization is used to minimize overfitting, and the regularization factor is set to 0.1 [24].

The performance of the trained deep network for rooftop extraction is assessed by applying it to the test scenes and comparing its predictions with the ground truth labels. To quantitatively evaluate the similarity between predicted and actual labels, accuracy and intersection over union (IOU) are employed as measurement metrics. These metrics are calculated according to Eqs. 2 and 3, where TP, FP, and FN are the numbers of true positives, false positives, and

false negatives, respectively.

$$Accuracy = \frac{TP}{TP + FN} \tag{2}$$

$$IOU = \frac{TP}{TP + FP + FN} \tag{3}$$

The results show that the trained deep network has an accuracy of 92.60% and an IOU of 87.38% on average in the test scenes of the DALES dataset, showing its satisfactory performance in rooftop extraction. Thus, the trained deep network can be applied to any area. We employ it in the extraction of rooftops from the second dataset. Figure 2 shows some examples of rooftop extraction from the second dataset. The boundaries of rooftops have been extracted and regularized using α-shape [1] and polyline compression [17] algorithms, respectively. The figure shows that rooftops have been effectively distinguished from other objects.

Fig. 2. Some identified rooftops. The underlying orthophoto serves solely for visualization purposes.

Subsequently, planar patches of rooftops are segmented using clustering, followed by region growing. The MDDC algorithm used for clustering normal vectors does not require prior knowledge regarding the dataset as input parameters, and it adaptively determines the shape and number of clusters in the data. The angle and height thresholds used in region growing were set to 7° and 10 cm. These values were obtained using trial and error in a small part of the dataset. Figure 3 shows plane segmentation results of some rooftops. It illustrates the effectiveness of the plane segmentation method in detecting roof faces. Small superstructures, such as vents and small chimneys, that are not identifiable as distinct planar segments appear as openings within the segments. In this way, the impact of superstructures can be considered in the identification of utilizable areas. By comparing the plane segmentation results with the ground truth data, the performance of plane segmentation is quantified in terms of accuracy and IOU. The assessment results show that the plane segmentation method has an accuracy of 98.69% and an IOU of 98.22%, suggesting that most planar segments have been accurately detected.

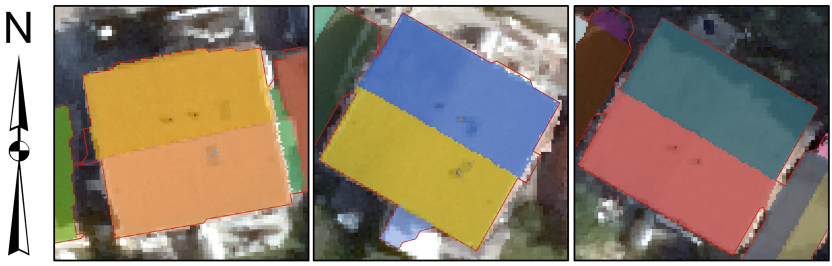

Fig. 3. The outcome of plane segmentation for some rooftops.

To effectively locate areas utilizable for photovoltaic deployment, a rooftop solar irradiation map is necessary, in conjunction with planar segments. This is attributed to the need for cost-efficiency, which discourages the installation of photovoltaic systems in regions with low solar irradiation. The solar irradiation of each segment is estimated using the solar model of ArcGIS Desktop [14,28]. The solar model incorporates viewshed analysis to account for shadowing effects. The viewshed analysis generates a Boolean image indicating the extent to which the sky is occluded by surrounding objects as seen from a certain place in the DSM. In addition to occlusion, the solar model takes into account site orientation, atmospheric effects, and variations in the sun's position, making it a reliable tool for estimating global solar irradiation. Figure 4 illustrates the annual global solar irradiation distribution across some rooftops, computed with ArcGIS Desktop. The impact of shadows cast by surrounding objects is evident in this figure.

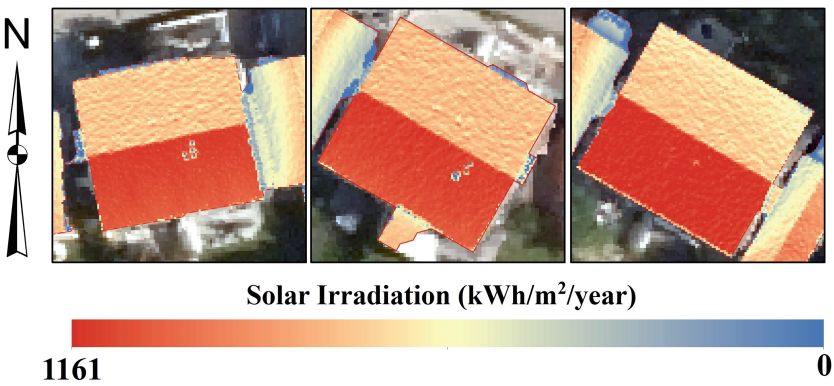

Fig. 4. Annual global solar irradiation of some rooftops.

Rooftop areas utilizable for solar panels are determined by excluding service areas, geometrically unsuitable areas, and areas with low solar irradiation. An erosion operation whose structuring element has a radius of 30 cm is used to remove service areas. Next, a series of opening operations are performed to

discard areas incapable of accommodating photovoltaic panels. The size of the structuring elements of opening operations is set to 1.7 m × 1.0 m, which is the common size of a commercial rooftop photovoltaic panel. Moreover, the solar irradiation threshold *SI* used to remove low-irradiated areas is set to 1000 kWh/m^2/year. Figure 5 shows the resulting utilizable areas of some rooftops in the dataset. The figure clearly illustrates how the methodology takes into account minor superstructures, indicated by white circles, when identifying utilizable areas. It also shows that buffers equivalent to the width of service areas have been removed from planar segments. Furthermore, some large planar segments have been removed due to insufficient solar irradiation. The approach successfully considers factors such as rooftop shape, orientation, superstructures, and occlusions when determining suitable areas for placing photovoltaics.

The study area encompasses a total rooftop area of 4224 m m^2, with 700 m^2 deemed utilizable. Annually, the entire rooftop area generates 403505 kWh of electricity, while the utilizable portions contribute 90105 kWh of electricity. The electricity yield has been estimated using Eq. 1, where the efficiency and performance ratio of the photovoltaics were set to 0.16 and 0.75, respectively. The utilizable areas account for only a small percentage of the total rooftops (16.6%); as a result, evaluating the solar energy potential of buildings based on their entire rooftop areas could result in overestimation.

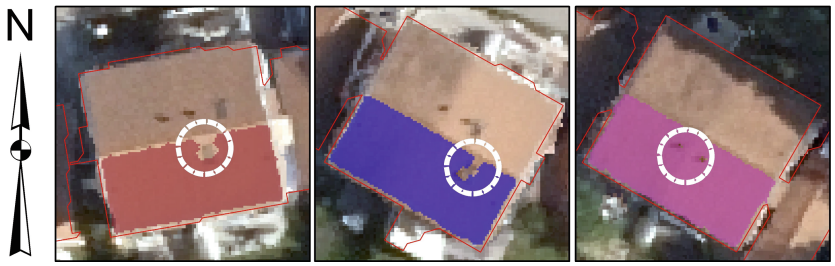

Fig. 5. Utilizable areas of some rooftops. The impact of superstructures is highlighted by white circles.

5 Conclusion and Future Work

Rooftop photovoltaics have acquired a prominent place in cities due to their potential to contribute to energy sustainability. They a have high capacity to reduce carbon emissions and environmental impacts of energy generation. Reliable assessments of rooftop solar potential require finding areas of rooftops where photovoltaics may be installed efficiently. In this study, a procedure was developed to estimate the solar energy potential of rooftops. First, rooftops were extracted from LiDAR point clouds using PointNet++, and their boundaries were regularized. Then, planar segments were extracted based on clustering

and region growing integration. The clustering step requires no prior knowledge regarding the dataset and has an optimized computational speed. In this step, planarity analysis was also incorporated to enhance clustering. Afterward, utilizable areas were determined by considering service areas, solar irradiation, roof shape, and occlusions. The results showed that rooftops and their planar segments were successfully extracted with 93% accuracy and 88% IOU and 99% accuracy and 98% IOU, respectively. In addition, it was observed that the shape, orientation, and superstructures of rooftops and shadow effects were satisfactorily considered in identifying utilizable areas. As a result, the procedure can be regarded as a reliable way to estimate the solar energy potential of rooftops in practice.

Although the methods have shown remarkable performance, there is still room for improvement. The economic feasibility of installing photovoltaics was not assessed in this study. The economic feasibility assessment involves estimating the costs and benefits of installation, such as the initial installation cost, maintenance expenses, and potential revenue from surplus power supplied to the grid. This assessment can aid in identifying the most economically viable rooftop areas for photovoltaics, considering both the potential for power production and the associated costs and benefits. Another potential direction is to extend the methods to include the façades of buildings. Our procedure focused only on rooftops and considered rooftops to be the only areas with the potential for installing photovoltaics. But façades of buildings can also have the suitable potential for generating energy. Thus, future work can extend our procedure to include façades in addition to rooftops.

References

1. Akkiraju, N., Edelsbrunner, H., Facello, M., Fu, P., Mücke, P., E., Varela, C.: Alpha shapes: definition and software. In: Proceedings on International Computational Geometry Software Workshop, Minneapolis (1995)
2. Aslani, M.: Computational and spatial analyses of rooftops for urban solar energy planning. Ph.D. thesis, Gävle University (2022)
3. Aslani, M., Seipel, S.: A fast instance selection method for support vector machines in building extraction. Appl. Soft Comput. **97**, 106716 (2020)
4. Aslani, M., Seipel, S.: Efficient and decision boundary aware instance selection for support vector machines. Inf. Sci. **577**, 579–598 (2021)
5. Aslani, M., Seipel, S.: A spatially detailed approach to the assessment of rooftop solar energy potential based on LiDAR data. In: The 8th International Conference on Geographical Information Systems Theory, Applications and Management, pp. 56–63. SCITEPRESS (2022)
6. Aslani, M., Seipel, S.: Automatic identification of utilizable rooftop areas in digital surface models for photovoltaics potential assessment. Appl. Energy **306**(Part A), 118033 (2022)
7. Benciolini, B., Ruggiero, V., Vitti, A., Zanetti, M.: Roof planes detection via a second-order variational model. ISPRS J. Photogram. Remote Sens. **138**, 101–120 (2018)

8. Bódis, K., Kougias, I., Jäger-Waldau, A., Taylor, N., Szabó, S.: A high-resolution geospatial assessment of the rooftop solar photovoltaic potential in the European Union. Renew. Sustain. Energy Rev. **114**, 109309 (2019)
9. Byrne, J., Taminiau, J., Kurdgelashvili, L., Kim, K.N.: A review of the solar city concept and methods to assess rooftop solar electric potential, with an illustrative application to the city of Seoul. Renew. Sustain. Energy Rev. **41**, 830–844 (2015)
10. Chen, D., Zhang, L., Mathiopoulos, P.T., Huang, X.: A methodology for automated segmentation and reconstruction of urban 3-D buildings from ALS point clouds. IEEE J. Sel. Topics Appl. Earth Obs. Remote Sens. **7**(10), 4199–4217 (2014)
11. Chow, A., Li, S., Fung, A.S.: Modeling urban solar energy with high spatiotemporal resolution: a case study in Toronto, Canada. Int. J. Green Energy **13**(11), 1090–1101 (2016)
12. Deschaud, J.E., Goulette, F.: A fast and accurate plane detection algorithm for large noisy point clouds using filtered normals and voxel growing. In: 3DPVT. Paris, France (2010)
13. Ester, M., Kriegel, H.P., Sander, J., Xu, X.: A density-based algorithm for discovering clusters in large spatial databases with noise. In: the Second International Conference on Knowledge Discovery in Databases and Data Mining, pp. 226–231. AAAI Press, Portland (1996)
14. Fu, P., Rich, P.M.: The Solar Analyst 1.0 Manual. Technical Report, Helios Environmental Modeling Institute (HEMI), USA (2000)
15. Gassar, A.A.A., Cha, S.H.: Review of geographic information systems-based rooftop solar photovoltaic potential estimation approaches at urban scales. Appl. Energy **291**, 116817 (2021)
16. Gilani, S.A.N., Awrangjeb, M., Lu, G.: segmentation of airborne point cloud data for automatic building roof extraction. GISci. Remote Sens. **55**(1), 63–89 (2018)
17. Gribov, A.: Optimal compression of a polyline while aligning to preferred directions. In: 2019 International Conference on Document Analysis and Recognition Workshops (ICDARW), vol. 1, pp. 98–102 (2019). https://doi.org/10.1109/ICDARW.2019.00022
18. Huang, Y., Chen, Z., Wu, B., Chen, L., Mao, W., Zhao, F., Wu, J., Wu, J., Yu, B.: Estimating roof solar energy potential in the downtown area using a GPU-accelerated solar radiation model and airborne LiDAR data. Remote Sens. **7**(12), 17212–17233 (2015)
19. Kingma, D.P., Ba, J.: Adam: a method for stochastic optimization. In: International Conference on Learning Representations (ICLR), Ithaca, San Diego (2015)
20. Lingfors, D., Bright, J.M., Engerer, N.A., Ahlberg, J., Killinger, S., Widén, J.: Comparing the capability of low- and high-resolution LiDAR data with application to solar resource assessment, roof type classification and shading analysis. Appl. Energy **205**, 1216–1230 (2017)
21. Lodha, S., Fitzpatrick, D., Helmbold, D.: Aerial lidar data classification using AdaBoost. In: Proceedings of the International Conference on 3-D Digital Imaging and Modeling, pp. 435–442. IEEE, Montreal, Canada (2007)
22. Lukač, N., Špelič, D., Štumberger, G., Žalik, B.: Optimisation for large-scale photovoltaic arrays' placement based on light detection and ranging data. Appl. Energy **263**, 114592 (2020)
23. Mainzer, K., Killinger, S., McKenna, R., Fichtner, W.: Assessment of rooftop photovoltaic potentials at the urban level using publicly available geodata and image recognition techniques. Solar Energy **155**, 561–573 (2017)
24. Murphy, K.P.: Machine Learning: A Probabilistic Perspective. MIT Press, Cambridge, Massachusetts (2012)

25. Nelson, J.R., Grubesic, T.H.: The use of LiDAR versus unmanned aerial systems (UAS) to assess rooftop solar energy potential. Sustain. Cities Soc. **61**, 102353 (2020)
26. Pavlidis, N.G., Hofmeyr, D.P., Tasoulis, S.K.: Minimum density hyperplanes. J. Mach. Learn. Res. **17**(156), 1–33 (2016)
27. Qi, C.R., Yi, L., Su, H., Guibas, L.J.: PointNet++: deep hierarchical feature learning on point sets in a metric space. In: 31st Conference on Neural Information Processing Systems (NIPS 2017), California (2017)
28. Rich, P., Dubayah, R., Hetrick, W., Saving, S.: Using viewshed models to calculate intercepted solar radiation: applications in ecology. In: American Society for Photogrammetry and Remote Sensing Technical Papers, pp. 524–529 (1994)
29. Romero Rodríguez, L., Duminil, E., Sánchez Ramos, J., Eicker, U.: Assessment of the photovoltaic potential at urban level based on 3D city models: a case study and new methodological approach. Solar Energy **146**, 264–275 (2017)
30. Rusu, R.B.: Semantic 3D Object Maps for Everyday Manipulation in Human Living Environments. Ph.D. thesis, Technical University of Munich, Munich, Germany (2009)
31. Sampath, A., Shan, J.: Segmentation and reconstruction of polyhedral building roofs from aerial LiDAR point clouds. IEEE Trans. Geosci. Remote Sens. **48**(3), 1554–1567 (2010)
32. Schallenberg-Rodríguez, J.: Photovoltaic techno-economical potential on roofs in regions and islands: the case of the canary islands. Methodological review and methodology proposal. Renew. Sustain. Energy Rev. **20**, 219–239 (2013)
33. Shin, Y.H., Son, K.W., Lee, D.C.: semantic segmentation and building extraction from airborne LiDAR data with multiple return using PointNet++. Appl. Sci. **12**(4), 1975 (2022)
34. Sundararajan, D.: Digital Image Processing A Signal Processing and Algorithmic Approach. Springer, Singapore (2017)
35. Thai, C., Brouwer, J.: Challenges estimating distributed solar potential with utilization factors: California universities case study. Appl. Energy **282**, 116209 (2021)
36. Thebault, M., Clivillé, V., Berrah, L., Desthieux, G.: Multicriteria roof sorting for the integration of photovoltaic systems in urban environments. Sustain. Cities Soc. **60**, 102259 (2020)
37. Varney, N., Asari, V.K., Graehling, Q.: DALES: a large-scale aerial LiDAR data set for semantic segmentation. In: 2020 IEEE/CVF Conference on Computer Vision and Pattern Recognition Workshops (CVPRW), pp. 717–726 (2020). https://doi.org/10.1109/CVPRW50498.2020.00101
38. Xie, Y., Tian, J., Zhu, X.X.: Linking points with labels in 3d: a review of point cloud semantic segmentation. IEEE Geosci. Remote Sens. Mag. **8**(4), 38–59 (2020)
39. Xu, Y., Stilla, U.: Toward building and civil infrastructure reconstruction from point clouds: a review on data and key techniques. IEEE J. Sel. Top. Appl. Earth Obser. Remote Sens. **14**, 2857–2885 (2021)
40. Yildirim, D., Büyüksalih, G., ahin, A.D.: Rooftop photovoltaic potential in Istanbul: calculations based on LiDAR data, measurements and verifications. Appl. Energy **304**, 117743 (2021)
41. Zheng, Y., Weng, Q.: Model-driven reconstruction of 3-d buildings using LiDAR data. IEEE Geosci. Remote Sens. Lett. **12**(7), 1541–1545 (2015)